



Wideband Slotted Planar Inverted-F Antenna using Eccosorb MCS Absorber for Millimeter-Wave Applications

Akhilesh Verma & N S Raghava*

Delhi Technological University, ECE Department, Delhi, India-110 042

Received 23 March 2021; accepted 28 April 2021

This work investigates the performance enhancement of the slotted planar inverted-F antenna (PIFA) using Eccosorb MCS absorber. In order to check the enhancement of the antenna performance, structure of the PIFA antenna with and without absorber has been analyzed. This antenna structure consists of two slots etched on the patch, which are placed at a height of $0.18\lambda_0$ from the substrate. We show that with the application of absorber, the radiation pattern can be transformed and produces the radiation beam in the desired direction. The proposed antenna is loaded with two layers of Eccosorb MCS absorber on the top of the substrate and with the other two layers below the substrate. Apart from providing radiation pattern in the desired direction, the antenna with absorber also provides wideband operation of 57.8 % bandwidth with high gain. The designs were first validated by simulations and then verified by measurements.

Keywords: PIFA Antenna, Eccosorb MCS absorber, Wideband, Millimeter-wave

1 Introduction

Wireless services are much affected due to heavy data traffic on the existing frequency bands. As mobile users are increasing day by day, the network congestion problem, call drops, and network unavailability are becoming biggest challenges for the users. One of the solutions to this problem is to move to higher band of frequencies as they provide wide bandwidth. In this regard, the mm-wave band is an interesting candidate as it has an unused wide spectrum. For upcoming fifth generation (5G) antennas, researchers are exploring mm-wave band which circumvent some of the above issues¹⁻².

The mm-waves range from 1-10 mm wavelength (10-100 GHz). While the mm-wave spectrum has many advantages, there are also some limitations that the researchers should be aware of. The tiny wavelength mm-waves are affected by raindrops, oxygen absorption, and line of sight during its propagation. The beam forming, beam splitting, and directive antennas are the key solutions to overcome these problems due to mm-waves. Mostly antennas are in the order of wavelengths and in this way short wavelengths of mm-wave allow the antennas that are compact as well as have high directivity³⁻⁴. The coverage of the desired direction with beam steering capability ranges from -90° to $+90^\circ$ in theta plane is obtained by three identical sub arrays of patch antennas

which are fed by switching to particular sub arrays reported in⁵. The radiation pattern at mm-wave is distorted by the scattering of the signals. Meanwhile, the damage of the patch antenna is controlled by placing conventional radome on the patch. But due to the comparable wavelength of the antenna with the radome thickness, the radiation pattern gets distorted, which reduced the radiation directivity of the antenna. The radiation pattern improvements, as well as high gain achieved by stacking of six pieces of the substrate, placed in a radome, but the reflection coefficient, get affected in⁶. A circular patch along with parasitic circular ring is used to obtain an ultra-wideband of 3.03 GHz bandwidth presented by Raghava *et al.*⁷. The performance of the microstrip patch antenna improved by stacking the two layers of the substrate in which one layer works as a reflector and the layer below the first one comprised of electronic band gap structure (EBG) by Raghava *et al.*⁸. It is also observed that the performance of the antenna is affected by air gap between the layers. An array of meta material is loaded in E-shaped microstrip patch antenna in which bandwidth is enhanced by 4 THz within 34.5-37.5 THz frequency band⁹. The dual-band six elements 28/38 GHz MIMO PIFA antenna is reported¹⁰, which achieved a bandwidth of 600 to 800 MHz at 28 GHz and 300 to 380 MHz at 38 GHz frequency band which is not enough for mm-wave applications. A wide bandwidth of 600 % is achieved in which the two segments of SRR Labyrinth metamaterial are loaded

*Corresponding author (E-mail: vakhilesh2015@gmail.com)

within the antenna structure¹¹. A swastika metamaterial based ultra-wideband antenna with proposed 400 % bandwidth is achieved and at the same time the 44 % size miniaturization is also obtained¹². Planar inverted-F antenna (PIFA) designed with slots having wide bandwidth ranges from 27.57 - 30.75 GHz, and peak gain of 8.3 dBi is reported¹³. The dimension of the substrate used is 110×60 mm which is large enough for mm-wave applications. The antenna covering 53GHz to 71GHz frequency band is proposed which achieved 29 % bandwidth and gain of 17.5 dBi¹⁴. The proposed antenna comprised an array of 4×4 patch antenna is fed by the L - probe. The radiation performance and reduction of surface waves are obtained through metal strips on the soft surface structure via fences. However, high gain with a tilted beam without using an array is reported¹⁵. The two L-shaped slots etched on the patch, which is fed by single coax feed, obtains two frequency bands of 28/38 GHz. The improvement of impedance matching and the axial ratio is achieved with the optimization of the slots¹⁶. However, the wide beam width between 100° and 125° is achieved by parasitic patches with multiple resonances and a wide bandwidth of 13 %, which covered 34.1 to 38.9 GHz frequency band through multi slotted microstrip patches were obtained¹⁷. The radiation pattern reconfigurability in respect of broadside radiation and end-fire radiation has been achieved by rectangular slots and dielectric loading respectively. The radiation pattern improvement has been carried out by varying number of slots¹⁸. Whereas, the conducting posts around the slot have been used to reduce the surface waves which help to improve the radiation pattern by removing the ripples in the E-plane pattern is observed and is reported¹⁹. It is observed²⁰, that the wide bandwidth along with high gain has been achieved through high impedance surfaces (HIS), which suppress the surface waves. The impedance bandwidth of 32 % (2.68 to 3.65 GHz) with 4.5 dBi gain is exhibited, which is improved value as compared to without HIS. The size of the antenna is $66 \times 66 \times 5.77$ mm³, which seems to be very large for wireless portable devices. 19.4 % bandwidth (4.69-5.7 GHz) and 7.32 dBi²¹ gain are achieved by using a layer of three substrates, and the top superstrate comprises of 7×7 square patch cells meta surface. The seamless and integration of other devices is difficult in the layered substrate for a wideband operation, which is overcome²² using 2×2 MIMO dual-band mm-wave monopole antenna.

In this manuscript, a combination of Eccosorb MCS²³ absorber in a slotted planar inverted-F antenna

(PIFA) is presented for mm-wave applications. The two shorting plates of different widths help to control the resonance frequency as well as impedance bandwidth of the antenna. In first antenna structure, after obtaining an optimized location of the absorber on and underneath the substrate, the nulls in bore sight direction of the radiation pattern are eliminated by loading the Eccosorb MCS absorber. The radiation pattern improvement, as well as wideband operation, is achieved with the absorber. The Eccosorb MCS absorber loaded substrate reduces the surface waves, which constructively enhances the bandwidth as well as the gain of the antenna.

2 Design of Slotted PIFA Antenna

The configuration of the proposed slotted planar inverted-F antenna is given in Fig. 1. The antenna has been designed on 1.6 mm thick RT/duroid substrate, having the dimensions of 20mm (Lg) \times 10mm (Wg). The dimensions of the patch are $0.90\lambda_0 \times 0.72\lambda_0 \times 0.32\lambda_0$ (λ_0 is calculated at frequency=27.3 GHz). The employed laminate has relative permittivity $\epsilon_r = 2.2$ and a dielectric loss tangent, $\tan(\delta) = 0.0009$, which are separated by the patch with a thickness of 0.035 mm. The air gap between the patch and the substrate is $0.18 \lambda_0$. The shorting plate SH₁ and SH₂ are soldered to both ends of the radiator to the ground at distances of F1 and F2 from the feed position. The distance between both shorting plates and feed helps to maintain the impedance of the antenna. The top copper radiator is fed by a 2.92 mm N-type connector. We will show later how the two slots ($l_s \times W_s$) etched on the radiator (see Fig. 1 (a)) and two stubs S1, S2 ($0.27 \lambda_0 \times 0.045 \lambda_0$) help to improve impedance bandwidth and affect the return loss.

The optimized parameters of the proposed antenna are shown in Fig. 1 i.e., LP = $0.90 \lambda_0$, WP = $0.72 \lambda_0$, W = 20 mm, X1 = 3 mm, X2 = 2 mm, a = 2 mm, X4 = 3 mm, Ws = 1.5 mm, ls = 6 mm, t = 2.5 mm, F1 = 6.4 mm and F2 = 8.6 mm respectively.

3 Design of Slotted PIFA Antenna Loaded with ECCOSORB MCS Absorber

The configuration of the absorber loaded slotted PIFA antenna is given in Fig. 2. The proposed design comprises of four strips of elastomeric microwave absorber on the top and bottom part of the substrate. The relative permittivity of the absorber is $\epsilon_r = 15$ and a loss tangent $\tan(\delta) = 0.002$. The size of absorber loaded PIFA antenna is $3.4 \lambda_0 \times 2.7 \lambda_0 \times 1.2 \lambda_0$ and the thickness of the absorber is 1 mm. The two

strips of the absorber are placed above the substrate having a gap of ‘Y2’ between them. The other two strips are placed on the bottom part of the substrate having a gap of ‘X3’ but near the other edge of the substrate.

4 Evolution of the Absorber Loaded PIFA Antenna

The geometry of the absorber loaded slotted PIFA antenna is evolved from the planar inverted-F antenna to achieve miniaturization and wideband, as shown in Figs. 3 & 4. Initially, the Ant1 consists of a narrow shorting plate where SH₁ shorts the narrow strip of the top radiator to the ground plane. The impedance of the antenna is controlled by the shorting plate as well as the distance between the feed and shorting plate. The obtained bandwidth of the antenna is 4.31 GHz covering 26.31-30.63 GHz band. The impedance of the antenna achieved $Z = 66.4+j3.3$. For further impedance matching, SH₁ is eliminated and a wide width shorting plate, SH₂ is shorted to the broad side of the radiator. Because of this wide width shorting plate, the bandwidth of 4.67 GHz is obtained. The impedance of the Ant2 is $Z = 54.7-j7.9$. After two steps of the antenna evolution,

two shorting plates are shorted at both ends of the radiator to the ground plane. In Ant3, an impedance of the antenna obtained is $53.9-j10.4$ and the operational bandwidth is 3.48 GHz, which covers 27.22-30.7 GHz band. Finally, evolved Ant4 resonates at 27.3 GHz, which covers 18.22-33.22 GHz band and achieved 15 GHz bandwidth. The impedance of the proposed Ant4 is $Z = 56.6+j3.4$ and impedance matching of $S_{11} \leq -10$ dB maintained throughout the band. It can be seen that the proposed antenna (Ant4) obtained good return loss and wide bandwidth as compared to other evolved antennas.

5 Parametric Analysis of Absorber Loaded Slotted PIFA Antenna

To study the effects of parameter variation on the performance of the antenna, a parametric analysis is done. The parametric analysis of the antenna is done with the high frequency structure simulator (HFSS). The length of the slot is varied from $l_s = 5$ mm to 7 mm and the other parameters $X_1, X_2, X_3, X_4, L_p, W_p, S_1, S_2, t, W, F_1, F_2, n, m, Y_1, Y_2, g_1, g_2, h_b, C_1, C_2$ kept constant. Fig. 5(a) shows that elongation of slot

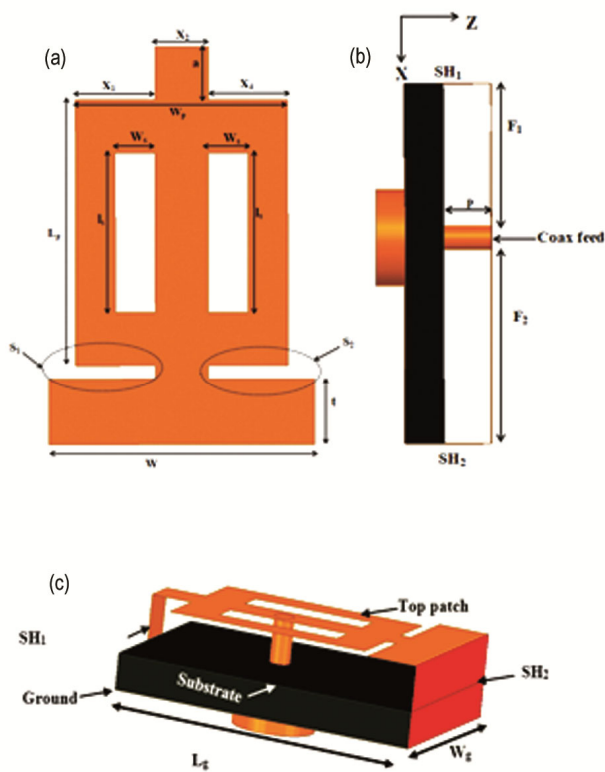


Fig. 1 — Geometry of the proposed slotted PIFA antenna (a) top view of the slotted patch, (b) side view (c) 3D view of the antenna.

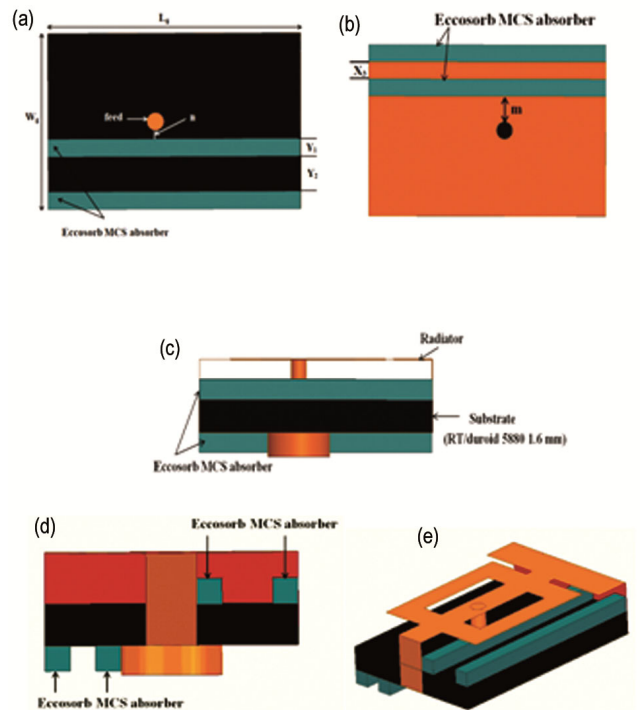


Fig. 2 — Geometry of the absorber loaded antenna (a) top view of the substrate, (b) bottom view (c) side view (d) front view (e) 3D view of the absorber loaded PIFA antenna ($L_g = 20$ mm, $W_g = 10$, $Y_1 = 1$, $Y_2 = 2$, $n = 0.5$, $X_3 = 1$, $m = 1.5$, units in mm).

improves the return loss at different frequencies and overall improves the impedance bandwidth. The length of slot of 6 mm is seen as appropriate for the structure which gives desired wideband response. Furthermore, the width of the slots W_s is varied at discrete values of 1.1, 1.5 & 1.9 mm with the rest of the parameters kept constant. It is observed that the slot width of 1.5 mm provides the wide bandwidth as compared to other dimensions of the slots as shown in Fig. 5b. While not shown here for brevity, but the lengths of both stubs S_1, S_2 affect the impedance of the antenna.

6 Simulated and Measured Results Discussion

A) S-Parameter

The photograph of the fabricated proposed antenna is shown in Fig. 6. The performance of the antenna

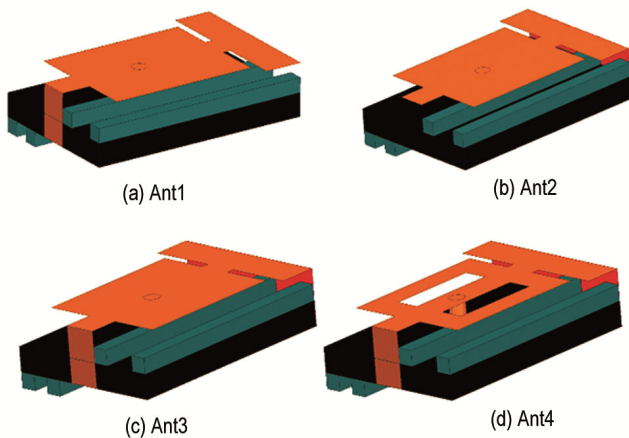


Fig. 3 — Evolutions of the proposed absorber loaded slotted PIFA antenna.

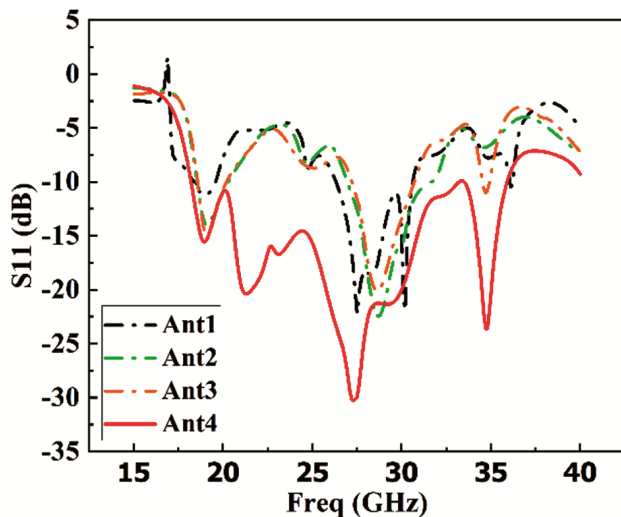


Fig. 4 — S-parameters for different evolutions of the proposed antenna.

is demonstrated by simulated and measured results. Fig. 7 shows the S-parameter comparison of the conventional PIFA and the Eccosorb MCS absorber loaded PIFA. It is observed that the PIFA antenna without absorber covers a frequency band from 24.88 to 26.39 GHz and obtained 5.89 % bandwidth. After loading the absorber in the slotted PIFA antenna, the bandwidth of the proposed antenna is increased by 57.8 %. The antenna is loaded with absorber extend the bandwidth due to the coupling between antenna and absorber. The frequency band covered by the absorber loaded PIFA antenna is 18.22 to 33.22 GHz,

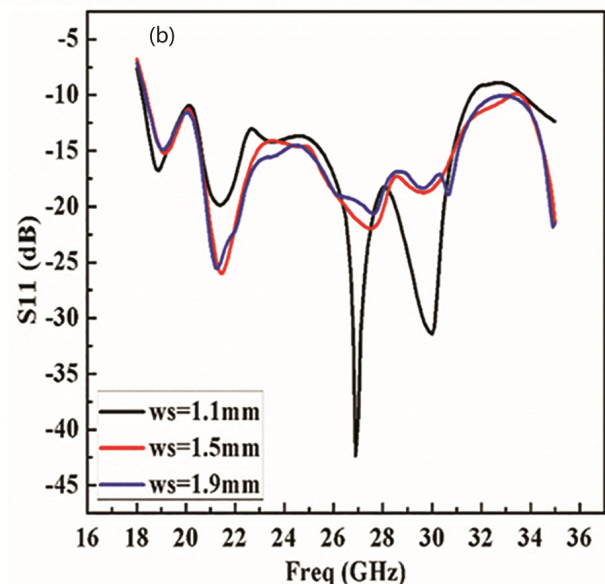
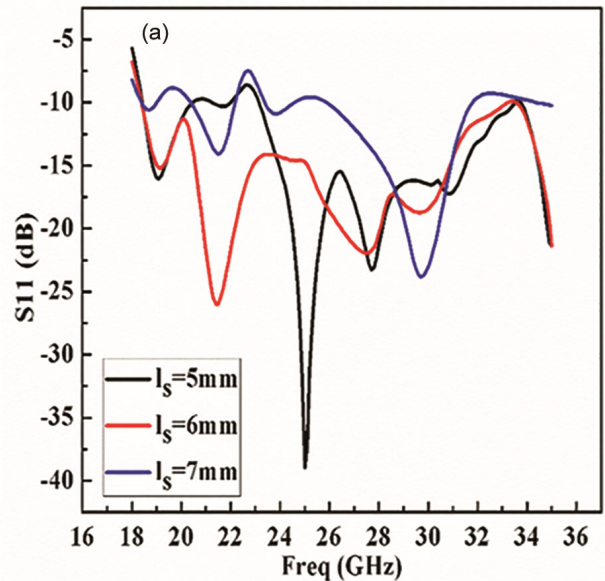


Fig. 5 — Parametric analysis of the proposed antenna (a) with slot length parametric analysis and, (b) with slot width parametric analysis.

which resonates at 27.3 GHz and it can be observed that the performance of the reflection coefficient is also improved. The simulated and measured S-parameter plot of the proposed antenna is shown in Fig. 8. The measured bandwidth of the proposed antenna is 42 %, which covers 19.7 to 30.32 GHz respectively. In summary, the loading of Eccosorb absorber in PIFA antenna plays an important role in bandwidth enhancement.

B) Radiation Pattern

Figure 9 exhibits the simulated 3D radiation patterns of the slotted PIFA with and without the absorber at 27.3 GHz. It is observed from Fig. 9a,



Fig.6 — Fabricated absorber loaded slotted PIFA antenna

slotted PIFA antenna without absorber has deep null in bore sight direction, however, after loading the absorber, deep null is completely eliminated and antenna achieves maximum radiation in bore sight direction. Adding Eccosorb MCS absorber to PIFA antenna, enhanced the gain, offered beam reflection. For better insights, radiation patterns are shown in 2D in Fig. 10 and can be seen that both measured and simulated patterns match well. The measured radiation patterns in E and H plane at 27.3 GHz compared with the simulations are shown in Fig. 10.

C) Gain

The realized gain of the antenna is shown in Fig. 11. We see that there is increase in the gain of the PIFA antenna once two strips of the absorber are placed on the substrate and other two strips are placed on the bottom near the other edge of the substrate which enhanced the gain of the antenna. It is also visible that the absorber loading gives the gain over the whole bandwidth of the antenna. The gain value of absorber loaded PIFA antenna is 7.3 dBi at 27.3 GHz. The simulated and measured value of the gain are in good agreement.

D) Surface current distribution analysis

Figure 12(a) shows the surface current on the antenna element. There are two slots in the patch antenna. Without absorber, the current distributed on the surface around the slots is symmetric. But, once the absorber is placed near one of the slots, the

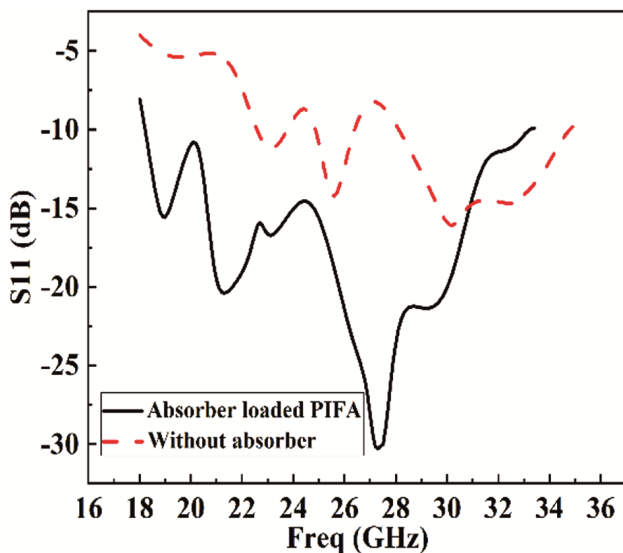


Fig. 7 — Simulated S11 of the proposed PIFA antenna.

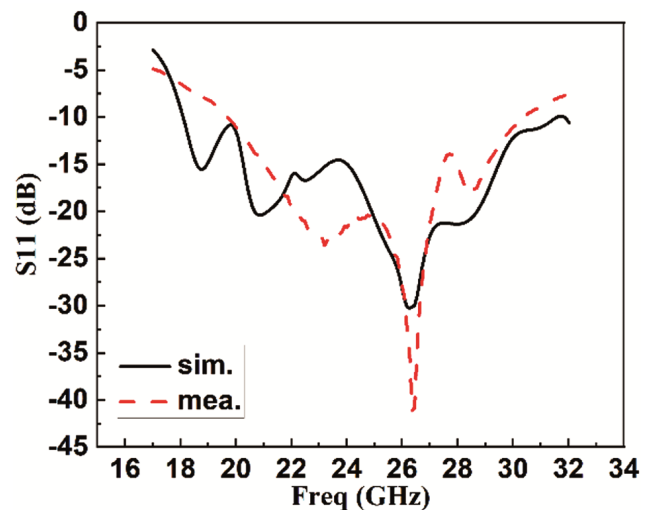


Fig. 8 — Simulated and measured S11 of the proposed absorber loaded PIFA antenna.

symmetry breaks as one of the slots is nearer to absorber as considered to other. This change in symmetry creates new distribution of surface current that is different when absorber was absent as shown in Fig. 12(b). Placement of absorber also creates surface current near the feed point which in turn will create new far field components. The new surface current distributions change the overall far field pattern that is different from the initial, without absorber, antenna as also visible in Fig. 9. Due to change of surface current distribution, the coupling

between slotted antenna and the absorber on both side of the substrate is enhanced which yields the wider bandwidth. The maximum current density on the radiator is 81.3 A/m in presence of absorber while it was 65.2 A/m when absorber was absent.

E) Performance of the proposed work

Table 1 shows the comparison between the proposed mm-wave antenna and previously published

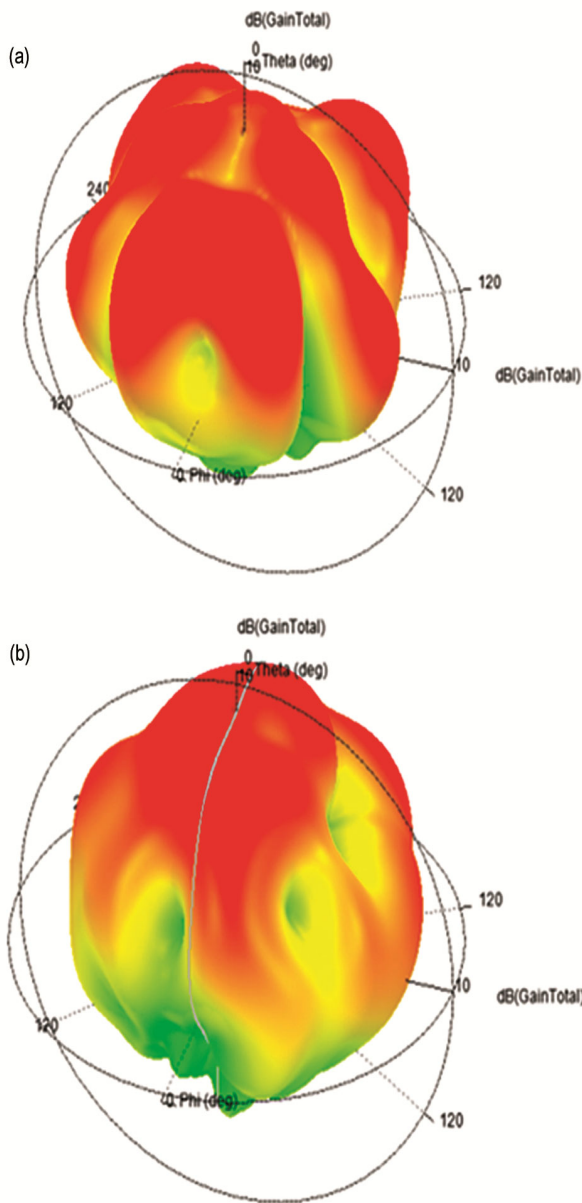


Fig. 9 — 3D radiation pattern of the antenna (a) without absorber (b) with absorber @ 27.3 GHz.

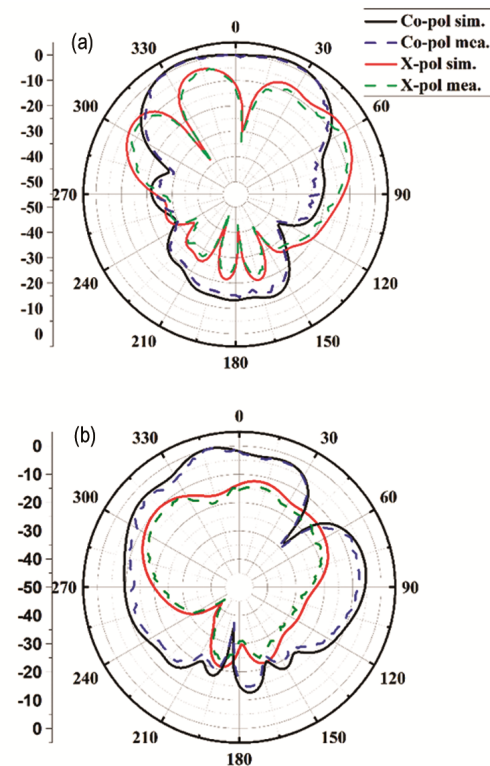


Fig. 10 — Simulated and measured radiation patterns of the proposed absorber loaded PIFA antenna @ 27.3 GHz (a) E-plane (b) H-plane.

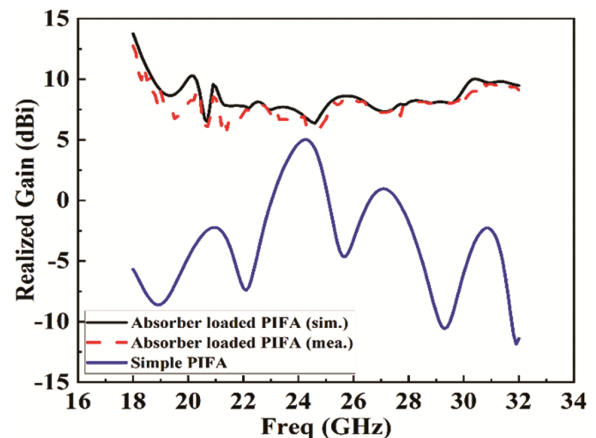


Fig. 11 — Gain of the proposed antenna.

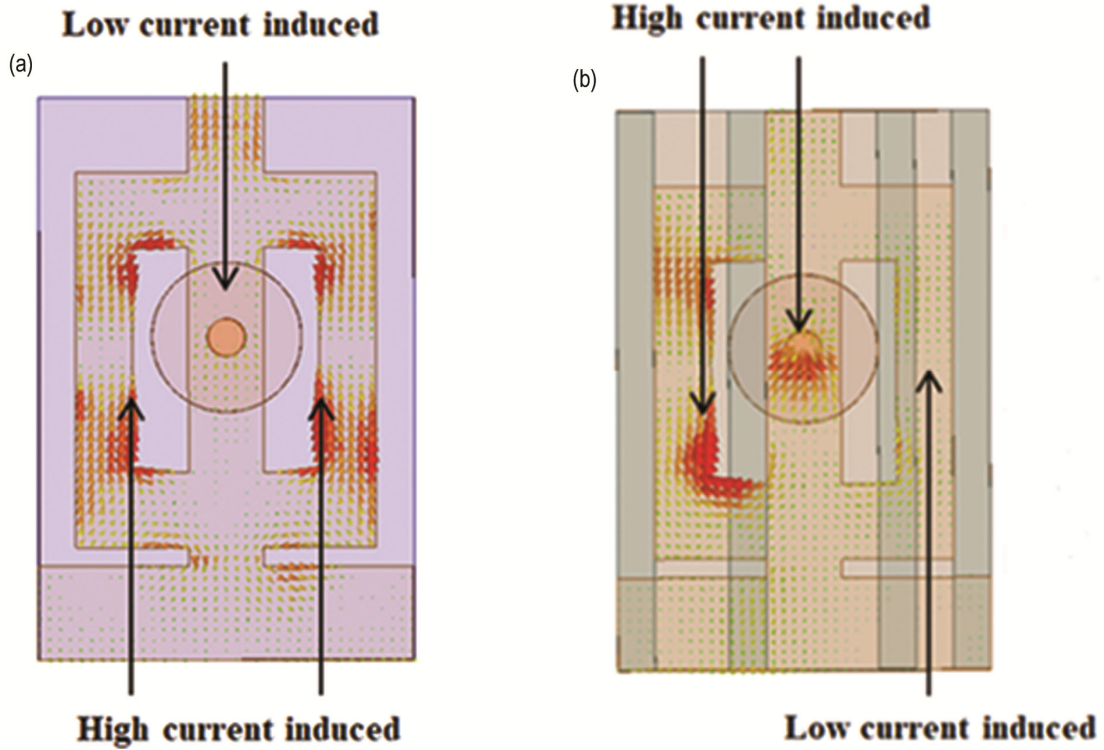


Fig. 12 — Surface current distribution of the proposed antenna (a) without absorber (b) with absorber

Table 1 — Comparison of the proposed antenna with previously reported work.

Ref	Freq. Band (GHz)	BW (GHz)	Size (mm ³)	Gain (dBi)	Effi. (%)	Elements
[4]	37	0.6	not given	10.8	not given	4
[5]	21.5	1	110 × 55 × 4.5	12.5	95	8
[6]	24	few MHz	11.5λ ₀ × 5.7λ ₀ × 0.47λ ₀ 3.78 × 5.66 × 77	7	not given	1
[10]	28	0.6-0.8	0.44λ ₀ × 0.67λ ₀ × 9.1λ ₀ 1.3 × 1.836 × 0.381	6.2/ 6.8	not given	6
[13]	28	27.57-30.75	0.12λ ₀ × 0.17λ ₀ × 0.035λ ₀ 4 × 4 × 1.34	8.8	97.9-98.9	1
[14]	60/70	53-71	0.56λ ₀ × 0.56λ ₀ × 0.18λ ₀ 14.4 × 14.4 × 1	17.5	85	16
[15]	28	26.9-29	6.8λ ₀ × 6.8λ ₀ × 0.47λ ₀ 30 × 19.9 × .79	7.4	not given	1
[16]	28/38	27.575-28.425	4.2λ ₀ × 2.76λ ₀ × 0.11λ ₀ 6.8 × 6.8 × 0.254	4	84/91	1
[17]	38	34.1-38.9	0.94λ ₀ × 0.94λ ₀ × 0.035λ ₀ 15.6 × 13 × 0.254	3.76	66.8	1
[18]	14.4/ 16.1	-	3.4λ ₀ × 2.8λ ₀ × 0.05λ ₀ 41 × 40 × 3.2	11.3/ 8.7	not given	1
[19]	17	16-18	2.9λ ₀ × 2.8λ ₀ × 0.02λ ₀ -	11.6	85	1
[20]	3	2.68-3.65	66 × 66 × 5.77	7.21	not given	1
[21]	5.2	4.69-5.7	1.32λ ₀ × 1.32λ ₀ × 0.12λ ₀ 9 × 8 × 4.5	7.8	96.2	1
[22]	28/38	26.65-29.2 36.95-39.05	0.25λ ₀ × 0.23λ ₀ × 0.13λ ₀ 14 × 12 × 0.38	1.27 1.83	78 76	2
Work1	26.36	19.7-30.32	13.6λ ₀ × 13.6λ ₀ × 0.16λ ₀ 10 × 8 × 3.6	7.3	94	1
			3.4λ ₀ × 2.7λ ₀ × 1.2λ ₀			

work in literature. The presented antenna provides not only better impedance bandwidth but also offers compact size with good gain throughout the desired frequency band compared to existing structures.

7 Conclusion

This paper proposed an absorber loaded PIFA antenna, where two strips of the absorbers are placed above the substrate and the other two strips of the absorbers are placed below the substrate. With the help of the absorbers, the null presented in boresight direction in case of conventional PIFA is removed and more radiation is created in boresight direction. The proposed absorber loaded PIFA antenna achieved 46.6 % size reduction as compared to the PIFA antenna without absorber. The absorber loaded PIFA antenna achieved a wide bandwidth of 57.8 %, which is an enhancement of 51.9 % as compared to the PIFA without absorber. Overall, proposed antenna is a good candidate for millimetre wave applications with good radiation properties.

References

- 1 Wells J, *IEEE Microw Mag*, 10 (2009) 104.
- 2 Shorbagy M E, Shubair R M, AlHajri M I & Mallat N K, *Mediterran Microw Symposium (MMS)*, (2016) 1.
- 3 Rappaport T S, Gutierrez F, Ben-Dor E, Murdock J N, Qiao Y & Tamir J I, *IEEE Trans Antennas Propag*, 61 (2013) 1850.
- 4 Chu H & Guo Y X, *IEEE Trans Compon Packaging Manuf Technol*, (2017) 964.
- 5 Ojaroudiparchin N, Shen M, Zhang S, Pedersen G F A, *IEEE Antennas Wirel Propag Lett*, 15 (2016) 1747.
- 6 Hong K D, Huang G L, Zhang X & Yuan T, *Cross Strait Quad-Regional Radio Sci Wirel Technol Conf (CSQRWC)*, (2019) 1.
- 7 Raghava N S, De A, Arora P, Malhotra S, Bazaz R, Kapur S & Manocha R, *IEEE Int Conf Commun Signal Process*, (2011) 276.
- 8 Raghava N S & De A, *Int J Microw Opt Technol*, 4 (2009) 315.
- 9 Dawar P, De A & Raghava N S, *Mater Res Innov*, 20 (2016) 240.
- 10 Hashem Y A, Haraz O M & El-Sayed E D M, *IEEE Int Symp Antennas Propag (APSURSI)*, (2016) 393.
- 11 Dawar P, Raghava N S & De A, *Int J Antennas Propag*, (2019).
- 12 Dawar P, Raghava N S & De A, *Int J Microw Opt Technol*, 11 (2016) 423.
- 13 Morshed K M, Esselle K P, Heimlich M, Habibi D & Ahmad I, *IEEE Region Symp (TENSYP)*, 10 (2016) 194.
- 14 Wang L, Guo Y X & Sheng W, *Asia Pacific Microw Conf Proceedings*, (2012) 151.
- 15 Park J S, Ko J B, Kwon H K, Kang B S, Park B & Kim D, *IEEE Antennas Wirel Propag Lett*, 15 (2016) 1685.
- 16 Aliakbari H, Abdipour A, Mirzavand R, Costanzo A, Mousavi P, *Eur Conf Antennas Propag (EuCAP)*, (2016) 1.
- 17 Kornprobst J, Wang K, Hamberger G & Eibert T F, *IEEE Trans Antennas Propag*, 65 (2017) 4293.
- 18 Agrawal T & Srivastava S, *Int J Electron Commun (AEÜ)*, 87 (2018) 70.
- 19 Faezi H, Kashani F H & Tayarani M, *Int J Electron Commun (AEÜ)*, 94 (2018) 84.
- 20 Panda P K & Ghosh D, *Int J Electron Commun (AEÜ)*, 111 (2019) 84.
- 21 Feng G, Shi X, Chen L, Yue H & Yang Y, *J Electromag Wave*, 31(2017) 1167.
- 22 Hasan Md N, Bashir S & Chu S, *J Electromag Wave*, 33 (2019) 1581.
- 23 <https://www.laird.com/products/absorbers/microwave-absorbing-elastomers-and-films/eccosorb-mcs>.